Science & Technology Development Journal, 24(SI1):SI18-SI24

Open Access Full Text Article

Research Article

A meshless radial point interpolation method for finite deformation analysis of hyperelasticity

Thai Van Vu[1,2], Vay Siu Lo[1,2], Hien Thai Nguyen[1,2], Nha Thanh Nguyen[1,2,*]

ABSTRACT

Hyperelastic materials are special materials that possess the non-linear material property. In these materials, the stress-strain relation is derived from the strain energy density function. An interesting property of these materials like rubber is the ability of elastic response when it is subjected to large deformations. That means when the load is removed, the material can easily return to the initial configuration. In addition, they also have some excellent mechanical properties like good tear and abrasion resistance, flexibility at ambient temperature. So hyperelastic materials are widely used in the industry. Due to this reason, it is needed to take a careful look at these materials, especially in the field of mechanical behavior. Because hyperelastic materials usually work under large deformation for almost all cases, their behavior is often considered in a highly non-linear elastic state. This paper presents a meshless radial point interpolation method for hyperelastic bodies with compressible and nearly-incompressible states. The weak form is obtained from the principle of minimum potential energy, and the finite deformation analysis of non-linear behavior is performed under the total Lagrange formulation. Radial point interpolation method shape functions are employed to approximate field nodes and derivatives. Due to possessing the Kronecker delta function property, the boundary conditions are imposed directly in the proposed method. Moreover, this method also shows its advantage for non-linear analysis, especially when the large deformation is considered and the highly-distorted nodal mesh is inherent in the structure. Two numerical examples are conducted with some distributed loads for both compressible and nearly-incompressible states. The obtained results show good agreement with the reference solution. That clearly demonstrates the efficiency and reliability of the proposed method for complex problems.

Key words: Large deformation, meshfree method, hyperelasticity

[1]*Department of Engineering Mechanics, Faculty of Applied Sciences, Ho Chi Minh City University of Technology, 268 Ly Thuong Kiet Street, District 10, Ho Chi Minh City, Vietnam*

[2]*Vietnam National University Ho Chi Minh City, Linh Trung Ward, Thu Duc City, Ho Chi Minh City, Vietnam*

Correspondence

Nha Thanh Nguyen, Department of Engineering Mechanics, Faculty of Applied Sciences, Ho Chi Minh City University of Technology, 268 Ly Thuong Kiet Street, District 10, Ho Chi Minh City, Vietnam

Vietnam National University Ho Chi Minh City, Linh Trung Ward, Thu Duc City, Ho Chi Minh City, Vietnam

Email: nhanguyen@hcmut.edu.vn

History

- Received: 2021-09-01
- Accepted: 2021-11-27
- Published: 2021-02-11

DOI : 10.32508/stdj.v24iSI1.3801

Check for updates

INTRODUCTION

Non-linear analysis is still a challenging issue in the field of computational mechanics due to its complexity. One of the typical representatives of non-linear problems is material nonlinearity, in which hyperelastic materials are representative. For example, rubber-like materials have non-linear mechanical responses under even small loads. Moreover, hyperelastic materials have also possessed some useful properties in the industry like supper deformation, high durability, and lightweight. High durability is the key factor for designers and buyers. So, it is necessary to evaluate the strength of parts which is made from the mentioned material in the structure.

There are various models of hyperelastic materials like neo-Hookean, Mooney-Rivlin, Yeoh, Ogden,… which are employed to describe the stress-strain relationship. But generally, hyperelastic materials are considered in large deformation conditions in which it seems to be impossible to find the correct solution. In this case, numerical methods are usually used to simulate the non-linear response of hyperelasticity. Along with the development of numerical methods, finite element methods (FEM) are very strong and popular in computational engineering. FEM has been widely used for complex engineering and science problems, including non-linear elastic problems [1–3]. However, FEM and other mesh-based methods have fallen into a disadvantage in the existence of the mesh of elements. Especially in the case of large deformation, the mesh of elements can be extremely distorted, and it can not produce a good approximation. To overcome the disadvantage of mesh-based methods, meshless methods have been developed to be independent of the nodal mesh to improve the accuracy of the solution on the highly distorted nodal mesh. There are some studies using the meshless method for simulating the finite deformation that have been performed and achieved significant results. Li *et al.* in [4] have proposed the reproducing kernel particle method (RKPM) for the large deformation problem of thin shell structures in 2000. The meshless local Petrov-Galerkin (MLPG) method was introduced by

Cite this article : Vu T V, Lo V S, Nguyen H T, Nguyen N T. **A meshless radial point interpolation method for finite deformation analysis of hyperelasticity**. *Sci. Tech. Dev. J.;* 24(SI1):SI18-SI24.

Han *et al.* for solving non-linear problems with large deformations and rotations[5], and large deformation contact analysis of elastomers[6]. In 2019, a strong-form mesh-free method for stress analysis of hyperelastic materials was presented by Khosrowpour *et al.*[7]. A meshless radial point interpolation method (RPIM) has been proposed for compressible states only by Nha *et al.*[8]. This study develops the RPIM method for large deformation analysis in both compressible and nearly-incompressible states of hyperelastic 2D problems. The weak form of the non-linear elastic problem is obtained from the principle of minimum potential energy[9]. To solve the non-linear equations, the Newton-Raphson algorithm is applied with a tolerance value of 10^{-6}.

The paper is constructed as follows. The constitutive laws for hyperelastic material models and RPIM meshless method for non-linear elasticity are presented in Section 2. Section 3 shows numerical examples and comparisons with the reference solution. Some issues are discussed in Section 4. Finally, Section 5 presents the main conclusions and remarks about the presented method.

METHODOLOGY

Constitutive equations of hyperelastic material

Consider a hyperelastic material that is subjected to forces. The geometry is changed from the undeformed to the deformed state. In the initial undeformed geometry, a particular point M is mapped into a point N in the current deformed geometry. These mentioned points are identified by vectors X and x, respectively. The deformation gradient tensor denoting the relation between X and x is defined as

$$F_{ij} = \frac{\partial x_i}{\partial X_j} = \frac{\partial u_i}{\partial X_j} + \delta_{ij} \tag{1}$$

Also, volume change between current and initial configuration is the determinant of deformation gradient tensor

$$J = det\,(F) \tag{2}$$

In addition, the right Cauchy-Green deformation tensor **C** and Lagrangian strain are introduced as follows

$$\begin{aligned} C &= F^T F \\ E &= \frac{1}{2}(C - I) \end{aligned} \tag{3}$$

where I is the identity matrix, the strain energy density function ψ can be constructed by deformation gradient tensor F. The second Piola-Kirchhoff stress S and the Cauchy stress (real stress) σ can be obtained by relationship as bellow

$$S = \frac{\partial \psi}{\partial E} = \frac{2\partial \psi}{\partial C};\ \sigma = \frac{1}{J} F S F^T \tag{4}$$

In this paper, the strain energy density function ψ obeys the neo-Hookean model[10]. This model has been considerably used to reproduce the mechanical response of rubber-like materials due to the good agreement with experiments. It was given as

$$\psi = \frac{\kappa}{2}(J-1)^2 + \frac{\mu}{2}\left[I_1 - 3 - 2\ln(J)\right] \tag{5}$$

where κ and μ are parameters of material (bulk and shear modulus, respectively). I_1 is the first invariant of the right Cauchy-Green deformation tensor. Based on Eq. (5), the non-linear stress-strain relation for the compressible neo-Hookean model can be written as

$$S = \kappa\left(J^2 - J\right)C^{-1} + \mu\left(I - C^{-1}\right) \tag{6}$$

In addition, the constitutive tensor D can be obtained by differentiating the second Piola-Kirchhoff stress S

$$D = \frac{\partial S}{\partial E} \tag{7}$$

Large deformation in RPIM method

Consider a hyperelastic solid denoted by the continuum domain Ω, subjected to external forces $\mathbf{t}^*$ on the boundary Γ_t, body force b, displacement u^* on the Γ_u boundary as shown in Figure 1.

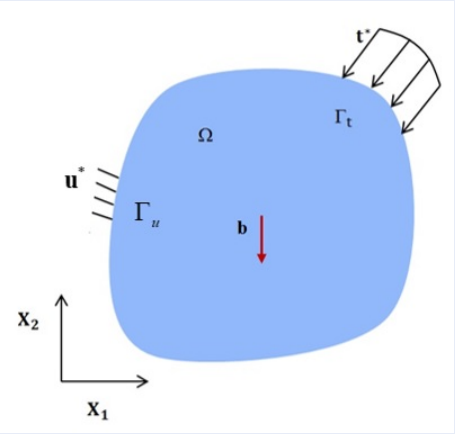

Figure 1: Boundary conditions of hyperelastic material

The potential energy can be obtained from the strain energy and work done by applied forces as

$$\begin{aligned} \Pi(u) &= \Pi^{int}(u) - \Pi^{ext}(u) \\ &= \int_\Omega W(E)\,d\Omega - \int_\Omega ubd\Omega - \int_\Omega ut^* d\Gamma \end{aligned} \tag{8}$$

The weak form of the non-linear elastic problem can be achieved from the principle of minimum potential energy

$$\int_\Omega S:\bar{E}d\Omega - \int_\Omega \bar{u}bd\Omega - \int_{\Gamma_t}\bar{u}^T t^* d\Gamma = 0 \quad (9)$$

where $\bar{u}$ is similar to virtual displacement in the principle of virtual work. With the non-linear state of weak form due to the effect of energy form, it is necessary to apply the linearization into Eq.(9). This leads to the following equation

$$\begin{aligned}&\int_\Omega \left(\bar{E}:D:\triangle E + S:\triangle\bar{E}\right)d\Omega\\&-\int_\Omega \bar{u}bd\Omega - \int_{\Gamma_t}\bar{u}^T t^* d\Gamma = 0\end{aligned} \quad (10)$$

In this paper, RPIM shape functions ϕ and nodal displacement in the local support domain are employed to approximate the displacement field u. For more details of RPIM shape functions, readers can refer to [11]. The approximation of displacement field u and $\bar{u}$ are written as

$$u = \sum_{i=1}^N \phi_i u_i;\ \ \bar{u} = \sum_{i=1}^N \phi_i \bar{u}_i \quad (11)$$

The variation of Largrangian strain $\bar{E}$ and the incremental Largrangian strain can be written as

$$\bar{E} = B\bar{d};\ \triangle\bar{E} = B\triangle\bar{d} \quad (12)$$

Where $\bar{d}$ is the variation of nodal displacements, and B is the non-linear displacement-strain matrix

$$\begin{aligned}&B_{3\times 2N} =\\&\begin{bmatrix} F_{11}\phi_{1,1} & F_{21}\phi_{1,1}\\ F_{12}\phi_{1,2} & F_{22}\phi_{1,2}\\ F_{11}\phi_{1,2}+F_{12}\phi_{1,1} & F_{21}\phi_{1,2}+F_{22}\phi_{1,1}\end{bmatrix}\\&\quad\cdots\qquad\quad\cdots\\&\begin{bmatrix} F_{11}\phi_{N,1} & F_{21}\phi_{N,1}\\ F_{12}\phi_{N,2} & F_{22}\phi_{N,2}\\ F_{11}\phi_{N,2}+F_{12}\phi_{N,1} & F_{21}\phi_{N,2}+F_{22}\phi_{N,1}\end{bmatrix}\end{aligned} \quad (13)$$

The first and the second term of energy form can be written as

$$\int_\Omega \bar{E}:D:\triangle E d\Omega = d^{-T}\left(\int_\Omega B^T DBd\Omega\right)\triangle d \quad (14)$$

$$\int_\Omega S:\triangle\bar{E}d\Omega = d^{-T}\left(\int_\Omega H^T \oplus Hd\Omega\right)\triangle d \quad (15)$$

where

$$H_{4\times 2N} = \begin{bmatrix}\phi_{1,1} & 0 & \ldots & \phi_{N,1} & 0\\ \phi_{1,2} & 0 & \ldots & \phi_{N,1} & 0\\ 0 & \phi_{1,1} & \ldots & 0 & \phi_{N,1}\\ 0 & \phi_{1,2} & \ldots & 0 & \phi_{N,2}\end{bmatrix} \quad (16)$$

$$\oplus_{4\times 4} = \begin{bmatrix}S_{11} & S_{12} & 0 & 0\\ S_{12} & S_{22} & 0 & 0\\ 0 & 0 & S_{11} & S_{12}\\ 0 & 0 & S_{12} & S_{22}\end{bmatrix} \quad (17)$$

So the energy form of weak form can be rewritten as

$$\begin{aligned}&\int_\Omega \left(\bar{E}:D:\triangle E + S:\triangle\bar{E}\right)d\Omega\\&= d^{-T}\left(\int_\Omega B^T DBd\Omega\right)\triangle d\\&\quad + d^{-T}\left(\int_\Omega H^T\oplus Hd\Omega\right)\triangle d\\&= d^{-T}\left[\left(\int_\Omega B^T DB + H^T\oplus H\right)d\Omega\right]\triangle d\\&= d^{-T}K\triangle d\ =\ d^{-T}f^{int}\end{aligned} \quad (18)$$

In addition, work done by applied forces can be approximated as

$$\begin{aligned}&\int_\Omega \bar{u}^T bd\Omega + \int_{\Gamma_t}\bar{u}^T t^* d\Gamma\\&= \sum_{i=1}^N \bar{u}_i^T\left\{\int_\Omega \phi_i bd\Omega + \int_{\Gamma_t}\phi_i t^* d\Gamma\right\}\\&= \bar{d}^T f^{ext}\end{aligned} \quad (19)$$

The difference between the left-and right-hand sides of Eq. (10) is defined as a residual and it can be solved by the Newton-Raphson method

$$R = \bar{d}^T\left(f^{ext} - f^{int}\right) \quad (20)$$

NUMERICAL EXAMPLES

Two numerical examples of compressible and nearly-incompressible states are presented in this section to analyze the large deformation of solids. With the purpose of validation, parameters and model of the material are chosen the same as [10], and the results then are compared with [10]. The bulk modulus is given as 120.291 N/mm^2 in the compressible state and 400889.806 N/mm^2 for the nearly-incompressible state. The shear modulus is assumed as 80.194 N/mm^2. In considering the accuracy of the non-linear solution, an error value of 10^{-6} is applied for the Newton-Raphson algorithm.

Inhomogeneous compression problem

In the first example, the inhomogeneous compression problem is studied. The objective of this problem is to investigate the stability of the result due to the high compression level. The problem is shown in Figure 2, a rectangular plate subjects a constant distributed force f. The horizontal displacement at the top edge and vertical displacement at the bottom edge is set to be zero. It should be noted that due to the symmetry, only half of the plate is studied.

The convergence analysis of this problem is conducted in vertical displacement of point M. to investigate the convergence rate of the proposed method, four nodal distributions are chosen. The percent of compression at point M is computed with four cases of distributed force for compressible (f = 50; 100; 150 and 200 N/mm^2) and nearly-incompressible states (f = 100; 150; 200 and 250 N/mm^2). Figure 3 and Figure 4 show

the rate of convergence. In these figures, the percent of compression at point M versus to the total number of nodes of compressible and nearly-incompressible states are plotted and compared with the variational differential quadrature (VDQ) [10] method that used 45 × 45 nodes for simulations.

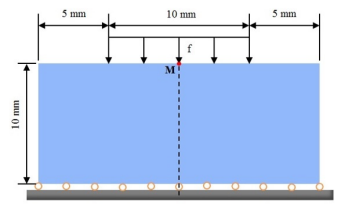

Figure 2: Inhomogeneous compression problem

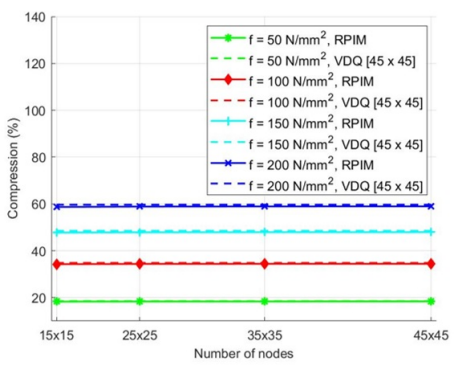

Figure 3: Percent of compression at point M for various values of distributed force in the compressible inhomogeneous compression problem

It is clear to see that the proposed method can produce a stable result of good accuracy. Like VDQ method, the convergence rate of the nearly-incompressible state is lower than the compressible state.

Figure 5 and Figure 6 show the deformed configurations of the plate under f = 200 N/mm^2 and f = 250 N/mm^2 for the compressible and nearly-incompressible state, respectively. The colors indicate values of the norm of stress $||P|| = \sqrt{P_{iI}P_{iI}}$ at each node

Figure 7 shows each component of the first Piola-Kirchhoff stress for compressible state with f = 200 N/mm^2.

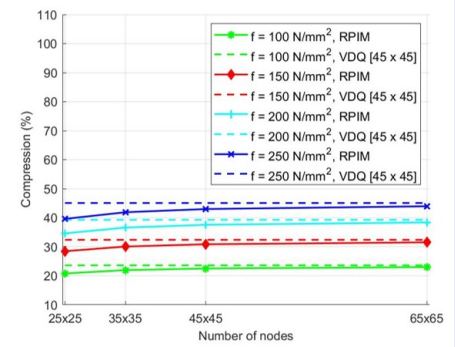

Figure 4: Percent of compression at point M for various values of distributed force in the nearly-incompressible inhomogeneous compression problem

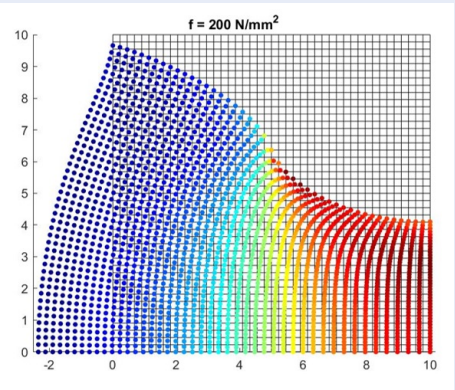

Figure 5: Deformed configuration of the plate in the compressible state with f = 200 N/mm^2 (black grid indicates the undeformed configuration of the plate)

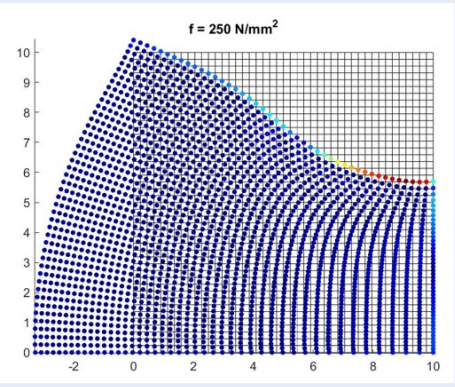

Figure 6: Deformed configuration of the plate in the nearly-incompressible state with f = 250 N/mm^2 (black grid indicates the undeformed configuration of the plate)

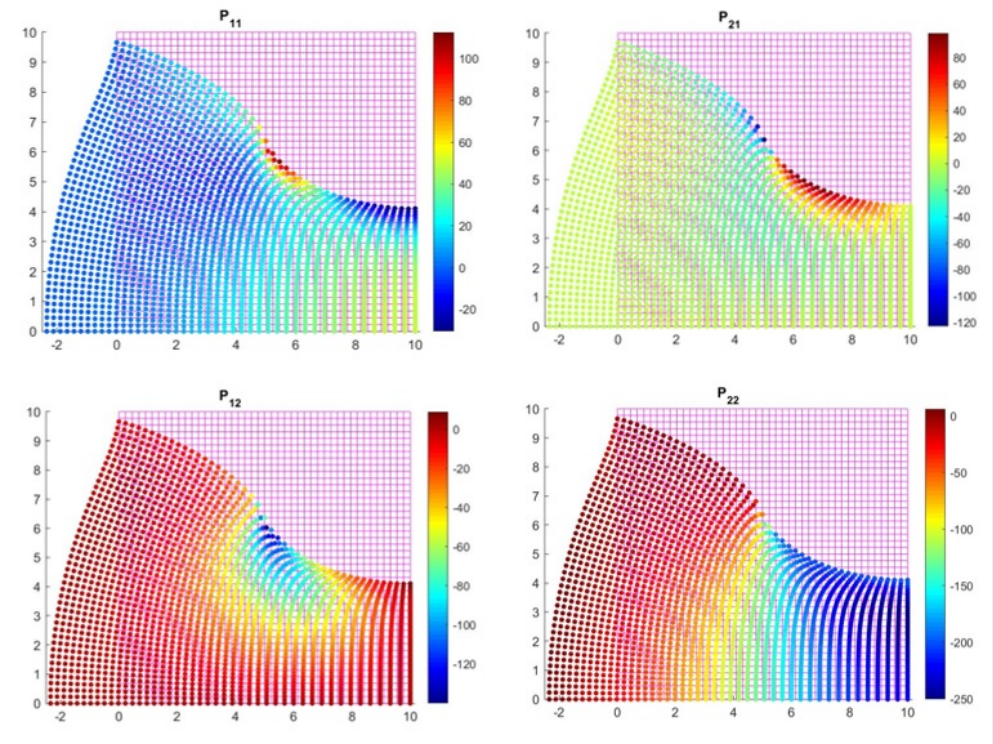

Figure 7: The first Piola-Kirchhoff stress in the compressible state with f = 200 N/mm^2

Curved beam problem

As the second example, a curved beam with a compressible state under bending load is considered. The geometry and load conditions are shown in Figure 8. The right edge is subjected to a constant distributed force while the bottom edge is clamped.

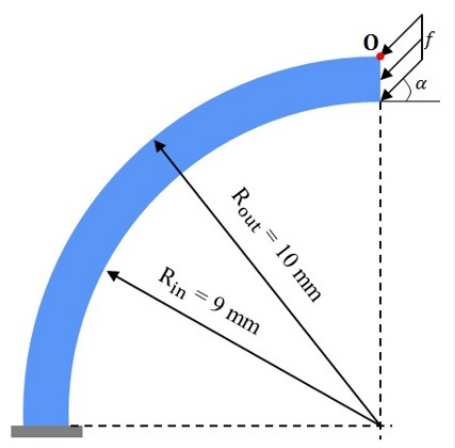

Figure 8: Curved beam problem

Similar to the previous example, the convergence analysis of this problem is performed in vertical displacement of point O under four values of distributed force (f = 0.2; 0.3; 0.4 and 0.5 N/mm^2). Figure 9 shows the vertical displacement of point O, and it is compared with the VDQ method that used 23 × 23 nodes for the simulation.

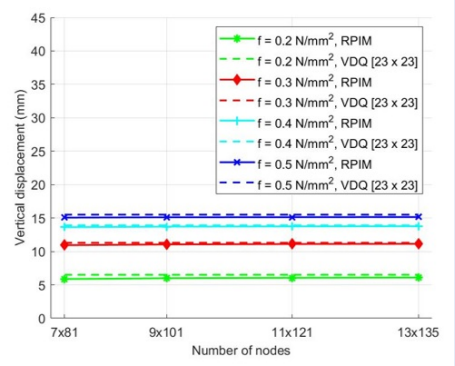

Figure 9: Vertical displacement at point M for various values of shearing force in the compressible curved beam problem

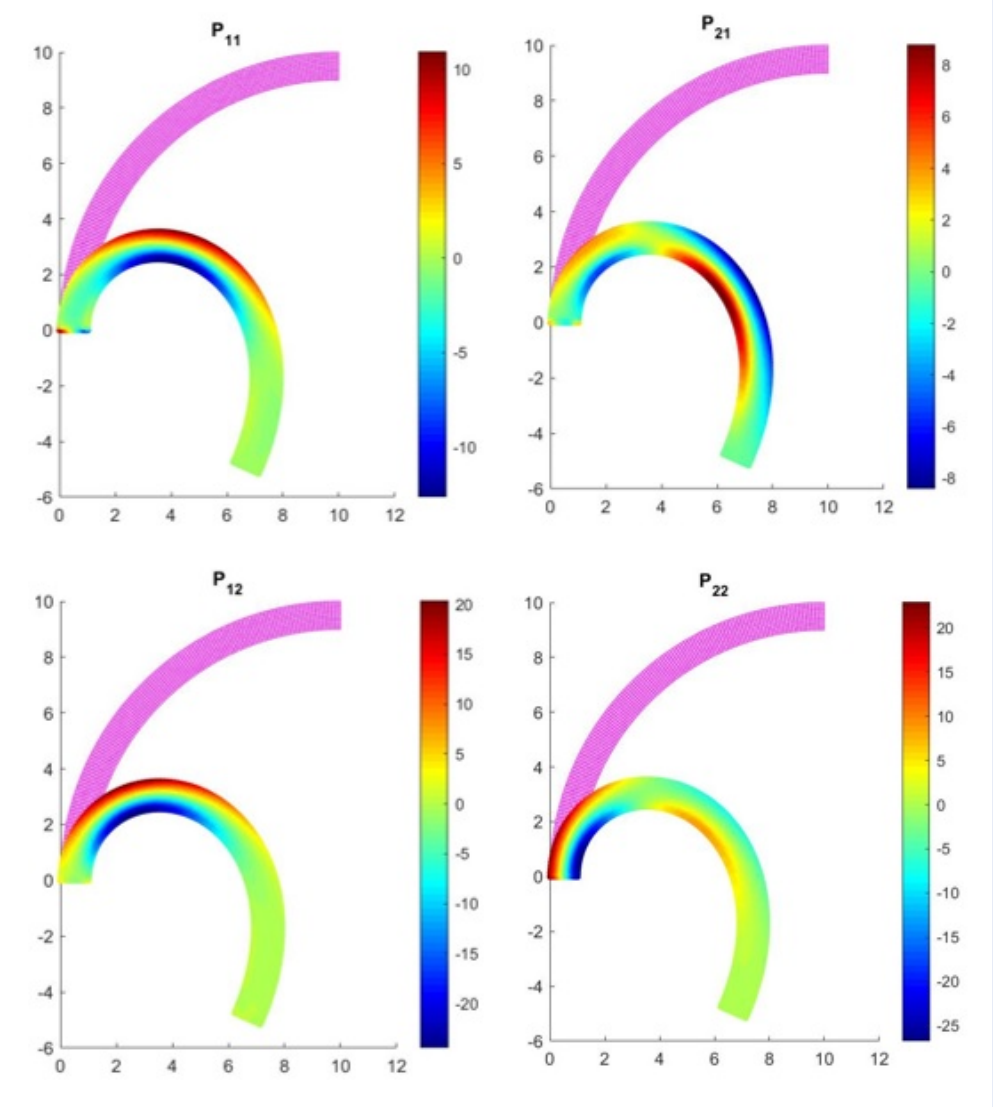

Figure 10: The first Piola-Kirchhoff stress in the compressible state with f = 0.5 N/mm^2

As expected, there is a good result given by the proposed method when compared with the VDQ method. Figure 10 shows each component of the first Piola-Kirchhoff stress with f = 0.5 N/mm^2.

DISCUSSION

As shown in Section 3, although the proposed method produces a good and stable solution for various problems of compressible and nearly incompressible behaviors in a simple way, some issues need to be discussed in this section. For example, in VDQ method, the fine mesh at edges is utilized for all cases while the regular node distribution in domains is employed to approximation in the RPIM method. Due to this, it also leads to using a smaller number of nodes in the VDQ method for some cases. Moreover, different from the proposed method, the energy function is discretized in a direct approach by the generalized differential quadrature operator in the VDQ method. Because of these reasons, there is a slight difference in the result compared with the reference solution.

CONCLUSION

In this paper, we have introduced a meshless method based on RPIM shape functions and successfully applied it to analyze the behavior of compressible and nearly-incompressible states of hyperelastic solid under finite deformation. The results under the high de-

formation level of the proposed method are compared with the VDQ method. As expected, they show validity with good accuracy and stable results. The proposed method does not need the mesh of elements, so there is no meshing task required, and distorted elements can not be generated when large deformation is considered. The meshless method seems full of hope and promise for advanced analysis such as fracture problems of hyperelastic materials in which the discontinuity is considered under large deformation. However, like the conventional meshfree methods, the proposed method still has some restrictions. One of them is the requirement of "the background cell" to perform the numerical integrations. In addition, determining the local support domain also affects the computation cost. These limitations should be improved in further studies.

ACKNOWLEDGMENT

We acknowledge the support of time and facilities from Ho Chi Minh City University of Technology (HCMUT), VNU-HCM, for this study.

ABBREVIATIONS

FEM: Finite Element Method
RPIM: Radial Point Interpolation Method
RKPM: Reproducing Kernel Particle Method
MLPG: Meshless Local Petrov-Galerkin
VDQ: Variational Differential Quadrature

CONFLICT OF INTEREST

The Group of authors declares that this manuscript is original, has not been published before, and there is no conflict of interest in publishing the paper.

AUTHOR CONTRIBUTION

Thai Van Vu works as the computational program developer and the manuscript editor.
Vay Siu Lo plays the role of algorithm builder.
Thai Hien Nguyen takes part in the work of gathering data.
Nha Thanh Nguyen is the supervisor of the group, and the one contributes ideas for the proposed method.

REFERENCES

1. Nomoto A, et al. 2-dimensional homogenization FEM analysis of hyperelastic foamed rubber. Procedia Engineering. 2016;147:431–436. Available from: https://doi.org/10.1016/j.proeng.2016.06.335.
2. Angoshtari A, Shojaei MF, Yavari A. Compatible-strain mixed finite element methods for 2d compressible non-linear elasticity. Computer Methods in Applied Mechanics and Engineering. 2017;313:596–631. Available from: https://doi.org/10.1016/j.cma.2016.09.047.
3. Ramabathira AA, Gopalakrishnan S. Automatic finite element formulation and assembly of hyperelastic higher order structural models. Apllied Mathematical Modelling. 2014;38:2867–2883. Available from: https://doi.org/10.1016/j.apm.2013.11.021.
4. Li S, et al. Numerical simulations of large deformation of thin shell structures. Computational Mechanics. 2000;25:102–116. Available from: https://doi.org/10.1007/s004660050463.
5. Han ZD, et al. Meshless Local Petrov-Galerkin (MLPG) Approaches for Solving Nonlinear Problems with Large Deformations and Rotations. CMES. 2005;10:1–12.
6. Hu D, et al. A meshless local petrov-galerkin method for large deformation contact analysis of elastomers. Engineering Analysis with Boundary Elements. 2007;31:657–666. Available from: https://doi.org/10.1016/j.enganabound.2006.11.005.
7. Khosrowpour E, et al. A strong-form meshfree method for stress analysis of hyperelastic materials. Engineering Analysis with Boundary Elements. 2019;109:32–42. Available from: https://doi.org/10.1016/j.enganabound.2019.09.013.
8. Nguyen NT, et al. An improved meshless method for finite deformation problem in compressible hyperelastic media. Vietnam Journal of MECHANICS. 2021;43(1). Available from: https://doi.org/10.15625/0866-7136/15332.
9. Kim NH. Introduction to Nonlinear Finite Element Analysis. Springer US, New York. 2015;.
10. Hassani R, et al. Large deformation analysis of 2D hyperelastic bodies based on the compressible non-linear elasticity: A numerical variational method. International Journal of Non-Linear Mechanics. 2019;116:39–54. Available from: https://doi.org/10.1016/j.ijnonlinmec.2019.05.003.
11. Nguyen NT, et al. Crack growth modeling in elastic solids by the extended meshfree Galerkin radial point interpolation method. Engineering Analysis with Boundary Elements. 2014;44:87–97. Available from: https://doi.org/10.1016/j.enganabound.2014.04.021.